Graubner, Tim; Karttunen, Antti J.; Kraus, Florian

A Dinuclear Uranium Complex $[\{UO_2F_2(NH_3)\}_2(\mu\text{-}F)_2]^{2-}$ from Reaction of TlF and UO_2F_2 in Liquid Anhydrous Ammonia and Fluoride Ion Affinities for Some Uranyl(VI) Species $[UO_2F_x]^{2-x}$ and $[UO_2F_x(NH_3)_{5-x}]^{2-x}$

Published in:
European Journal of Inorganic Chemistry

DOI:
10.1002/ejic.202300387

Published: 02/10/2023

Document Version
Publisher's PDF, also known as Version of record

Chemistry Europe
European Chemical Societies Publishing

WILEY VCH

Excellence in Chemistry Research

Announcing our new flagship journal

- Gold Open Access
- Publishing charges waived
- Preprints welcome
- Edited by active scientists

Meet the Editors of *ChemistryEurope*

Luisa De Cola
Università degli Studi di Milano Statale, Italy

Ive Hermans
University of Wisconsin-Madison, USA

Ken Tanaka
Tokyo Institute of Technology, Japan

EurJIC
European Journal of Inorganic Chemistry

Research Article
doi.org/10.1002/ejic.202300387

Chemistry Europe
European Chemical Societies Publishing

www.eurjic.org

Special Collection

A Dinuclear Uranium Complex $[\{UO_2F_2(NH_3)\}_2(\mu\text{-}F)_2]^{2-}$ from Reaction of TlF and UO_2F_2 in Liquid Anhydrous Ammonia and Fluoride Ion Affinities for Some Uranyl(VI) Species $[UO_2F_x]^{2-x}$ and $[UO_2F_x(NH_3)_{5-x}]^{2-x}$

Tim Graubner,[a] Antti J. Karttunen,[b] and Florian Kraus*[a]

UO_2F_2 abstracts F^- anions from TlF in liquid ammonia solution and the compound $[Tl_2(NH_3)_6][\{UO_2F_2(NH_3)\}_2(\mu\text{-}F)_2]$ is formed. The compound has been characterized by single crystal X-ray diffraction, Raman spectroscopy and quantum-chemical calculations for the solid state. Quantum-chemical investigation of the $[\{UO_2F_2(NH_3)\}_2(\mu\text{-}F)_2]^{2-}$ anion showed that the U–(μ-F)–U σ-3c-4e-bond is essentially ionic. The $[Tl_2(NH_3)_6]^{2+}$ cation shows a thallophilic Tl···Tl interaction. Fluoride ion affinities (FIAs) were calculated for different UO_2^{2+} species $[UO_2F_x]^{2-x}$ and $[UO_2F_x(NH_3)_{5-x}]^{2-x}$ with $x = 0$ to 4.

Introduction

The aqueous chemistry of uranyl(VI) fluorides plays an important role in the processing of radioactive waste as well as for the fate of U compounds in the environment. Therefore, in depth knowledge of the chemical species involved is necessary for both dissolved and solid compounds.[1,2] Unfortunately, structural characterization of the latter is often limited due to the lack of crystallization from aqueous solutions or because of crystals unsuitable for diffraction experiments are obtained.[1] Liquid anhydrous ammonia, aNH_3, is a solvent similar to water. However, crystallization from it is often better and leads to compounds that should be closely related to those from aqueous solutions but can be characterized by diffraction.[3] So far, only the ammonolysis of the compounds UO_2X_2 (X = F, Cl, Br, I, OAc, $^1/_2$ SO_4) has been studied.[4–9] There, these compounds show the tendency to form different ammine complexes of the UO_2^{2+} cation. In the case of UO_2F_2, the chemically hard fluorido ligands cannot be displaced by the chemically softer NH_3 ligands and the neutral complex compound $[UO_2F_2(NH_3)_3]$ is obtained instead.[8] In the heavier halides UO_2Cl_2 and UO_2Br_2, the halide anions are completely displaced by NH_3 molecules and pentagonal bipyramidal ammine complexes $[UO_2(NH_3)_5]^{2+}$ are obtained.[8,9] This coordination motif is very frequent in uranyl(VI) chemistry. Besides these pseudo-binary uranyl(VI) compounds UO_2X_2 (X = F, Cl, Br, I, OAc, $^1/_2$ SO_4) also the compound $Cs[UO_2(NO_3)_3]$ containing the complex $[UO_2(NO_3)_3]^-$ anion has been reacted with excess aNH_3 in presence of UF_4. Surprisingly, a reduction of U(VI) to U(V) was observed as the compound $[UO_2(NH_3)_5]NO_3 \cdot NH_3$ was obtained, containing a pentagonal bipyramidal $[UO_2(NH_3)_5]^+$ monocation,[10] while the other reaction products remained unidentified.

Investigations on the UO_2^{2+} cation acting as an F^- acceptor have only mainly been carried out for the aqueous system.[11] It was mentioned that the UO_2^{2+} cation is a strong F^- acceptor, able to abstract a F^- anion from the $[BF_4]^-$ anion,[12] but as of today, no quantitative values for its fluoride ion affinity (FIA) have been published.[13,14] In general, ionic fluorides are only little soluble or even insoluble in aNH_3 as the lattice energies of fluorides are very high in general and the quite temperature-dependent dielectricity constant of NH_3 is much smaller than the one of water.[3,15–18] To increase the solubility of fluorides in liquid NH_3, it is necessary to add promoters which accept F^- ions. First attempts were successful using $TiCl_3$ or $[SiF_4(NH_3)_2]$.[19,20] In a reaction of the latter with TlF in aNH_3 solution, the cation $[Tl_2(NH_3)_6]^{2+}$ was observed together with the formation of the $[SiF_6]^{2-}$anion.[20] We also reported on a reaction of $Cs[UO_2(NO_3)_3]$ with CuF_2 in liquid aNH_3, where the UO_2^{2+} cation reacts as an F^- acceptor to form $Cs[UO_2F_3(NH_3)_2]$.[21] Therefore, we conducted experiments with TlF and UO_2F_2 in aNH_3 and present now another example of an uranyl(VI) compound reacting as an F^- acceptor in liquid aNH_3.

Results and Discussion

From the reaction of UO_2F_2 with one equivalent of TlF in liquid aNH_3 at +40 °C under autogenous pressure, we obtained small

[a] T. Graubner, Prof. Dr. F. Kraus
Anorganische Chemie mit Ausrichtung Fluorchemie, Fachbereich Chemie
Philipps-Universität Marburg
Hans-Meerwein-Str. 4, 35032 Marburg (Germany)
E-mail: F.kraus@uni-marburg.de
Homepage: http://www.uni-marburg.de/de/fb15/arbeitsgruppen/anorganische_chemie/ag-kraus

[b] Prof. Dr. A. J. Karttunen
Department of Chemistry and Materials Science
Aalto University
Kemistintie 1, FI-02150 Espoo (Finland)

Supporting information for this article is available on the WWW under https://doi.org/10.1002/ejic.202300387

Special Collection Part of the Wöhler Vereinigung für Anorganische Chemie Prize Winners Special Collection.

Research Article
doi.org/10.1002/ejic.202300387

yellow plate-shaped crystals (Figure 1) which were of suitable size for the diffraction experiment after ten months of crystallization time. Single crystal structure analysis led to the composition $[Tl_2(NH_3)_6][\{UO_2F_2(NH_3)\}_2(\mu\text{-}F)_2]$ for these crystals and the formation of the compounds can be described by Equation (1).

$$2\ UO_2F_2 + 2\ TlF + 8\ NH_3 \rightarrow [Tl_2(NH_3)_6][\{UO_2F_2(NH_3)\}_2(\mu\text{-}F)_2] \quad (1)$$

This reaction can be understood as an ammonolysis reaction of the starting materials and it had been already shown that the "full" ammonolysis product of UO_2F_2 is $[UO_2F_2(NH_3)_3]_2 \cdot 2NH_3$, according to Equation (2).[8]

$$UO_2F_2 + 8\ NH_3 \rightarrow [UO_2F_2(NH_3)_3]_2 \cdot 2NH_3 \quad (2)$$

The $[\{UO_2F_2(NH_3)\}_2(\mu\text{-}F)_2]^{2-}$ anion of the title compound may be considered as an intermediate of this "full" ammonolysis as two equivalents of NH_3 per U atom are needed for the "full" conversion to the $[UO_2F_2(NH_3)_3]_2$ complex.

The $[\{UO_2F_2(NH_3)\}_2(\mu\text{-}F)_2]^{2-}$ anion presented here is one of the few examples of an ammine complex where the corresponding aqua complex is known which had been obtained as the Cs salt in the crystalline compound $Cs_2[\{UO_2F_2(H_2O)\}_2(\mu\text{-}F)_2]$.[22–26]

Bis(triamminethallium(I)) di(μ-fluorido)bis(amminedifluoridodioxidouranate(VI)), $[Tl_2(NH_3)_6][\{UO_2F_2(NH_3)\}_2(\mu\text{-}F)_2]$, crystallizes in the triclinic crystal system, in space group $P\bar{1}$ (no. 2) with the lattice parameters $a = 8.1547(5)$, $b = 8.3371(4)$, $c = 8.8667(5)$ Å, $\alpha = 62.177(2)°$, $\beta = 69.676(2)°$, $\gamma = 87.666(2)°$, $V = 494.55(5)$ Å^3 and $Z = 1$, at 100 K. For details of the structure determination and selected crystallographic data see Table 1 and the Supporting Information.

Table 1. Selected crystallographic data and details of the structure determination of $[Tl_2(NH_3)_6][\{UO_2F_2(NH_3)\}_2(\mu\text{-}F)_2]$.

Compound	$[Tl_2(NH_3)_6][\{UO_2F_2(NH_3)\}_2(\mu\text{-}F)_2]$
Formula	$Tl_2U_2F_6N_8O_4H_{24}$
Molar mass [g·mol^{-1}]	1199.07
Space group (No.)	$P\bar{1}$ (no. 2)
a [Å]	8.1547(5)
b [Å]	8.3371(4)
c [Å]	8.8667(5)
α [°]	62.177(2)
β [°]	69.676(2)
γ [°]	87.666(2)
V [Å^3]	494.55(5)
Z	1
Pearson symbol	*aP22* (w/o H atoms)
$\rho_{calc.}$ [g·cm^{-3}]	4.026
μ [mm^{-1}]	32.638
Color	yellow
Crystal morphology	block
Crystal size [mm^3]	0.106×0.100×0.093
T [K]	100
λ [Å]	0.71073 (MoK$_\alpha$)
No. of reflections	3011
θ range [°]	2.693–30.523
Range of Miller indices	$-10 \le h \le 11$ $-10 \le k \le 11$ $0 \le l \le 12$
Absorption correction	numerical
T_{max}, T_{min}	1.000, 0.627
R_{int}, R_σ	0.0475, 0.0191
Completeness of the data set	0.996
No. of unique reflections	3011
No. of parameters, restraints, constraints	105, 0, 0
S (all data)	1.269
$R(F)$ ($I \ge 2\sigma(I)$, all data)	0.0170, 0.0175
$wR(F^2)$ ($I \ge 2\sigma(I)$, all data)	0.0433, 0.0435
Extinction coefficient	0.0051(3)
Twin ratio	0.0766(9)
$\Delta\rho_{max}$, $\Delta\rho_{min}$ [e·Å^{-3}]	2.689, −1.466

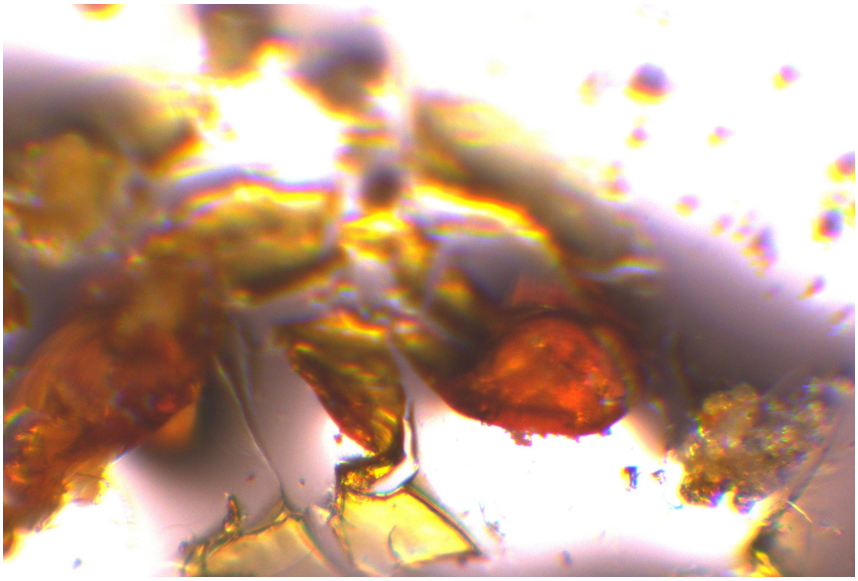

Figure 1. Photograph of the yellow plate-shaped crystals of $[Tl_2(NH_3)_6][\{UO_2F_2(NH_3)\}_2(\mu\text{-}F)_2]$ and an unidentified orange precipitate. Photo taken through the glass wall of the bomb tube at room temperature. Picture by Tim Graubner. Magnification factor of 5.

Research Article
doi.org/10.1002/ejic.202300387

The crystal structure contains one symmetry-independent Tl atom (2*i*, 1) which builds up the dinuclear $[Tl_2(NH_3)_6]^{2+}$ dication (C_i). The Tl···Tl distance of 3.8756(4) Å is slightly elongated compared with the reported one of 3.8546(8) Å in $[Tl_2(NH_3)_6][SiF_6]$ but still indicative of a thallophilic interaction.[20] Calculations on the compound using solid-state density functional theory at the DFT-PBE0/TZVP level of theory lead to a Tl···Tl distance of 3.7647 Å, which is only slightly shorter compared to the experimental distance. We showed previously that this dication is an example for thallophilic interactions,[20] so its electronic situation and Tl···Tl bond will not be discussed here.

The Tl–N bonds within the $[Tl(NH_3)_3]^+$ subunit of the cation show lengths of 2.541(3), 2.712(4) and 2.754(4) Å, which are slightly elongated in comparison to the previously reported ones of 2.521(3) and 2×2.614(2) Å.[20] The results from DFT calculations are with 2.551–2.701 Å in line with the experimental findings. While the shorter Tl–N bonds belong to the NH_3 ligands trans to the Tl···Tl axis, the longer Tl–N bonds belong to the other two NH_3 ligands.

Each $[Tl(NH_3)_3]^+$ subunit is surrounded by two $[\{UO_2F_2(NH_3)\}_2(\mu\text{-}F)_2]^{2-}$ anions as shown in Figure 2.

Compared to the coordination sphere of the Tl atoms in $[Tl_2(NH_3)_6][SiF_6]$ with coordination number C.N. = 3 + 2 + 1, which results from three NH_3 ligands, two F atoms of anions, and the neighboring Tl atom, the coordination sphere of the Tl atom in the title compound is different, see Figure 2, with a C.N. = 3 + 1 + 4 + 1, forming a strongly distorted tricapped trigonal prismatic coordination polyhedron. The inner coordination sphere is equal with three NH_3 ligands, the next sphere contains only one F atom which is terminally bound to the U atom of the $[\{UO_2F_2(NH_3)\}_2(\mu\text{-}F)_2]^{2-}$ anion. The third sphere consists of one O atom and a bridging μ-F atom belonging to the same $[\{UO_2F_2(NH_3)\}_2(\mu\text{-}F)_2]^{2-}$ anion as above. The second anion also coordinates with a bridging and a terminally bound F atom, however, its O atom does not contribute to the coordination sphere of the Tl atom. The interacting Tl atom is in the last sphere. In total, the dinuclear $[Tl_2(NH_3)_6]^{2+}$ cation is surrounded by four anions. The atomic distance between the Tl atom and the terminally bound F atom is 3.2892(2) Å, which is slightly elongated compared to the respective distance in the compound $[Tl_2(NH_3)_6][SiF_6]$ with 3.2454(18) Å. The distances to the O atom, two bridging F atoms, and another terminal F atom of the $[\{UO_2F_2(NH_3)\}_2(\mu\text{-}F)_2]^{2-}$ anion range from 3.5463(3) to 3.7783(2) Å. This significantly different coordination sphere of the Tl atoms with C. N. = 9 compared to the one in $[Tl_2(NH_3)_6][SiF_6]$ with C. N. = 6 is also a plausible reason why the Tl···Tl distance is elongated. In case of the title compound, the anions act both as bidentate and as tridentate ligands. The latter, that is, tridentate coordination with an uranyl O atom, a terminally bound, and a bridging F atom, seems to be a novel coordination motif. It has not been observed for the related aqua complex in the compound $Cs_2[\{UO_2F_2(H_2O)\}_2(\mu\text{-}F)_2]$. In this aqua complex, the C.N. of the Cs^+ cation is eleven, as it is coordinated by six F atoms and five O atoms which belong to five $[\{UO_2F_2(H_2O)\}_2(\mu\text{-}F)_2]^{2-}$ anions. The $[\{UO_2F_2(H_2O)\}_2(\mu\text{-}F)_2]^{2-}$ anion acts as a combination of a monodentate, bidentate and tridentate ligand.

The $[\{UO_2F_2(NH_3)\}_2(\mu\text{-}F)_2]^{2-}$ anion (C_i), shown in Figure 3, contains one symmetry-independent U atom (2*i*, 1) which is surrounded by seven atoms to form a pentagonal bipyramid-like coordination sphere with the O atoms forming the tips. This coordination sphere is well known for uranyl(VI) cations.[8–10,21] The U≡O distances agree with 1.787(3) and 1.796(3) Å compared to 1.781 and 1.783 Å in the $[\{UO_2F_2(H_2O)\}_2(\mu\text{-}F)_2]^{2-}$ anion and to 1.772(3) and 1.784(2) Å in the compound $[UO_2F_2(NH_3)_3]_2 \cdot 2NH_3$.[8,23] Despite the coordination of one of the O atoms to a Tl^+ cation, we observe no significant lengthening of the U≡O bond.

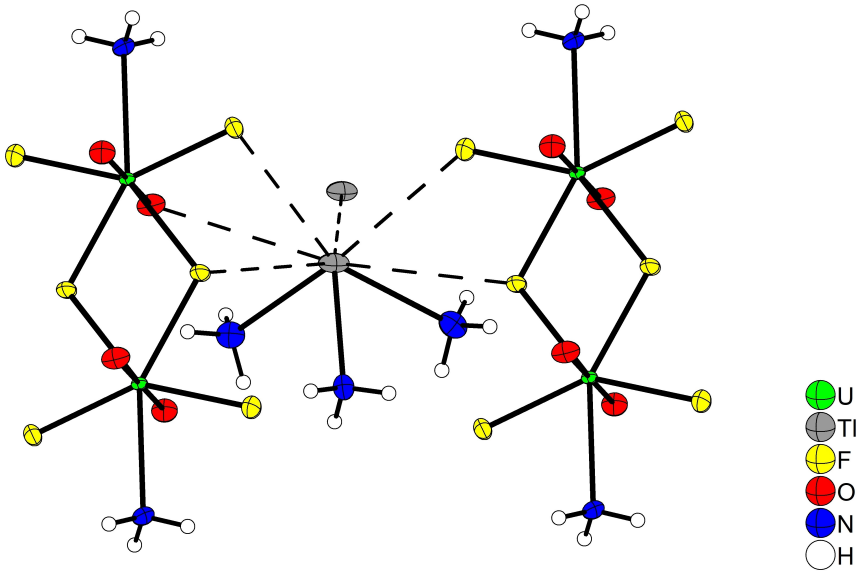

Figure 2. Section of the crystal structure of $[Tl_2(NH_3)_6][\{UO_2F_2(NH_3)\}_2(\mu\text{-}F)_2]$ illustrating the coordination sphere of a Tl atom. Atoms are shown with anisotropic displacement ellipsoids at the 70% probability level at 100 K and H atoms shown isotropic with arbitrary radii.

Research Article
doi.org/10.1002/ejic.202300387

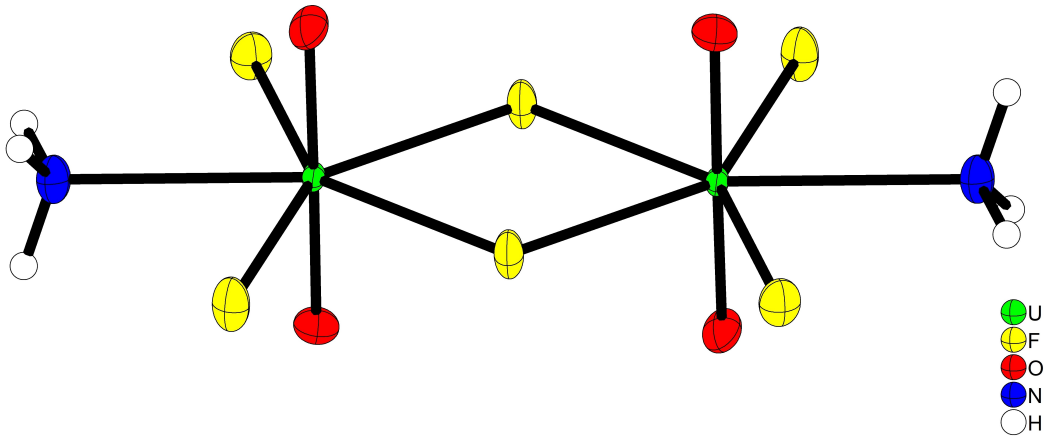

Figure 3. Structure of the molecular anion $[\{UO_2F_2(NH_3)\}_2(\mu\text{-}F)_2]^{2-}$ in the solid state. Atoms are shown with anisotropic displacement ellipsoids at the 70% probability level at 100 K and H atoms are shown isotropic with arbitrary radii.

The U≡O bond lengths from solid-state DFT calculations vary between 1.772–1.780 Å and are in agreement with the experimental values. The observed U–N bond length of 2.550(3) Å agrees with those in $[UO_2F_2(NH_3)_3]_2 \cdot 2NH_3$ with 2.526(4) to 2.549(4) Å and also with the DFT calculation which resulted in a bond length of 2.542 Å. The U–F bond lengths of the terminally bound F atoms are with 2.211(2) and 2.212(2) Å in agreement with those observed for $[UO_2F_2(NH_3)_3]_2 \cdot 2NH_3$ with 2.217(2)–2.241(2) Å, as well as 2.22 Å in the $[\{UO_2F_2(H_2O)\}_2(\mu\text{-}F)_2]^{2-}$ anion.[8,23] The DFT calculated bond lengths agree with 2.217–2.226 Å. In comparison to the terminally bound F atoms, the bridging μ-F atoms show, due to their higher coordination number, elongated U–(μ-F) bond lengths of 2.356(2) and 2.357(2) Å, as expected. This observation concurs with the solid state DFT calculations with 2.356 and 2.364 Å, as well as with 2.38 Å in the $[\{UO_2F_2(H_2O)\}_2(\mu\text{-}F)_2]^{2-}$ anion. The major difference between the anion of the title compound $[\{UO_2F_2(NH_3)\}_2(\mu\text{-}F)_2]^{2-}$ and the related aqua complex $[\{UO_2F_2(H_2O)\}_2(\mu\text{-}F)_2]^{2-}$ is the position of the coordinating solvato ligand. In the $[\{UO_2F_2(NH_3)\}_2(\mu\text{-}F)_2]^{2-}$ anion the solvato ligands reside trans to each other and trans to the U···U axis, see left side of Figure 6. The terminal F atoms are also trans arranged. In contrast, the solvato ligands in the $[\{UO_2F_2(H_2O)\}_2(\mu\text{-}F)_2]^{2-}$ anion reside trans to each other, while the terminal F atoms are cis-placed, see right side of Figure 6. Quantum-chemical studies on the energetic differences of these coordination isomers with NH_3 or H_2O ligands are discussed below.

As also in many other ammine compounds, hydrogen bonds are present, leading to additional interactions between the constituting ions. There are bi- and trifurcated hydrogen bonds from NH_3 ligands of the cation to the O and F atoms of the anion. Additionally, there are hydrogen bonds between the NH_3 ligand of the anion to a terminal F atom of another anion. Figure 4 shows the hydrogen bonds present in the crystal structure.

The F atoms of the anion act as acceptors of hydrogen bonds from the NH_3 ligands of the $[Tl_2(NH_3)_6]^{2+}$ cation with N···F distances of 2.960(4) to 3.085(4) Å and N–H···F angles from 156.2° to 168.2°, which is in agreement with the values reported for the compound $[Tl_2(NH_3)_6][SiF_6]$.[20] The N···O distances range from 3.137(4) to 3.200(4) Å with N–H···O angles between 166.1° to 171.4°. These values agree with those for $[UO_2F_2(NH_3)_3]_2 \cdot 2NH_3$.[8] More details are given in the Supporting

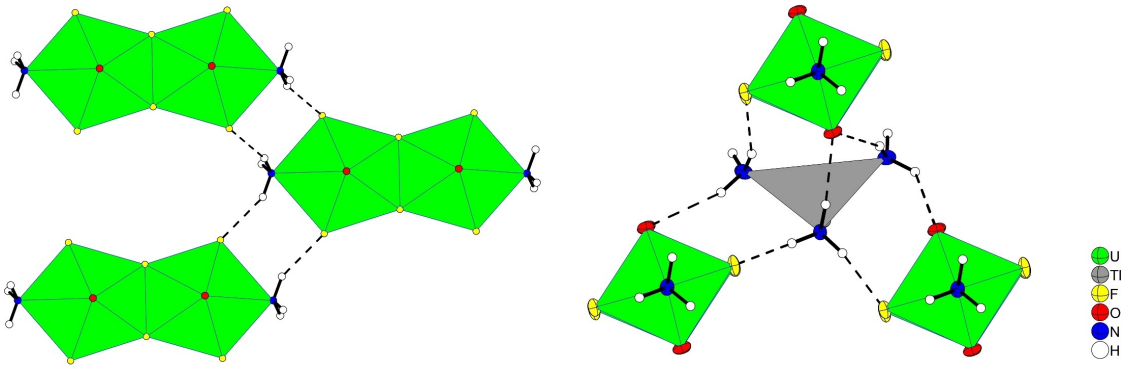

Figure 4. Section of the crystal structure of $[Tl_2(NH_3)_6][\{UO_2F_2(NH_3)\}_2(\mu\text{-}F)_2]$ showing the N–H···F/O hydrogen bonds. Left: Hydrogen bonds between the $[\{UO_2F_2(NH_3)\}_2(\mu\text{-}F)_2]^{2-}$ anions. Right: Hydrogen bonds between the $[Tl(NH_3)_3]^+$ subunit and three $[\{UO_2F_2(NH_3)\}_2(\mu\text{-}F)_2]^{2-}$ anions. Hydrogen bonds are shown as dashed lines, the ions are shown as polyhedra, and the atoms are shown with arbitrary radii.

Research Article
doi.org/10.1002/ejic.202300387

Information. Overall, the hydrogen bonds lead to the formation of a three-dimensional network within the crystal structure.

The global crystal structure may be viewed as an AB type structure related to the NaCl structure type. Both the centers of gravities of the $[Tl_2(NH_3)_6]^{2+}$ cations and those of the $[\{UO_2F_2(NH_3)\}_2(\mu\text{-}F)_2]^{2-}$ anions form distorted cubic closed packings with the respective other counterions in the octahedral voids. The pseudo-cubic unit cell is shown in Figure S1.

A recorded Raman spectrum of the yellow crystals of the title compound is compared in Figure 5 with the results of a solid-state calculation at the DFT-PBE0/TZVP level of theory. The calculation shows an overall agreement with the experiment.

Due to the rule of mutual exclusion only the A_g modes are Raman active, so no term symbols of modes will be explicitly discussed in the following. All bands were assigned via visualization of the vibrational normal modes. The characteristic U≡O stretching mode was observed at 812 cm^{-1} and 896 cm^{-1}, which is red-shifted compared to the band of UO_2F_2 with 975 cm^{-1}, see Figure S4. This redshift is expected as there are two additionally bound F atoms decreasing the electron density of the U≡O bond as well as the twofold negative charge of the anion which also leads to a weakening of the bond. Of the two observed U≡O stretching modes, one is described best with an asymmetric stretching vibration with respect to the inversion center in the center of the $[\{UO_2F_2(NH_3)\}_2(\mu\text{-}F)_2]^{2-}$ anion. The band is calculated at 873 cm^{-1} belonging to the band observed at 812 cm^{-1}. The second one calculated at 930 cm^{-1} is the symmetric stretching mode with respect to the inversion center, which was observed at 869 cm^{-1}. The bands observed in the region from 1092 to 1127 cm^{-1} correspond to the δ-wagging modes of the NH_3 ligands of the $[Tl_2(NH_3)_6]^{2+}$ cations. The mode at 1226 cm^{-1} is the δ-wagging mode of the NH_3 ligands of the $[\{UO_2F_2(NH_3)\}_2(\mu\text{-}F)_2]^{2-}$ anions. The bands in the region around 1602 cm^{-1} belong to the δ-rocking modes of the NH_3 ligands of the $[Tl_2(NH_3)_6]^{2+}$ cations and $[\{UO_2F_2(NH_3)\}_2(\mu\text{-}F)_2]^{2-}$ anions. Details are listed in Table S2. The high energy modes between 3175 and 3358 cm^{-1} correspond to the ν-stretching modes of the NH_3 ligands of the $[Tl_2(NH_3)_6]^{2+}$ cations and $[\{UO_2F_2(NH_3)\}_2(\mu\text{-}F)_2]^{2-}$ anions.

After removal of residual liquid NH_3 at room temperature (298 K), TlF and an unidentified crystalline species was observed by powder X-ray diffraction. UO_2F_2 was not observed. A recorded infrared spectrum of the residue shows a pronounced mode at 746 cm^{-1}. It is unclear what this band is due to as it would be a too large redshift for the U≡O band. In comparison, the IR shift of the U≡O band of the title compound, calculated at the DFT level of theory for the solid-state, is 934 cm^{-1}.

Quantum-Chemical Calculations

As mentioned above, the related aqua complex anion $[\{UO_2F_2(H_2O)\}_2(\mu\text{-}F)_2]^{2-}$ has a different bonding motif than the anion of the title compound. Within the structure of the $[\{UO_2F_2(NH_3)\}_2(\mu\text{-}F)_2]^{2-}$ anion, the terminal F atoms on each of the U atoms reside *trans* to each other being separated by the NH_3 ligands, see Figure 6 left. In contrast, the terminal F atoms at the U atoms of the aqua complex anion $[\{UO_2F_2(H_2O)\}_2(\mu\text{-}F)_2]^{2-}$ are *cis*-arranged with the H_2O ligands next to the bridging μ-F atoms, see the right of Figure 6.

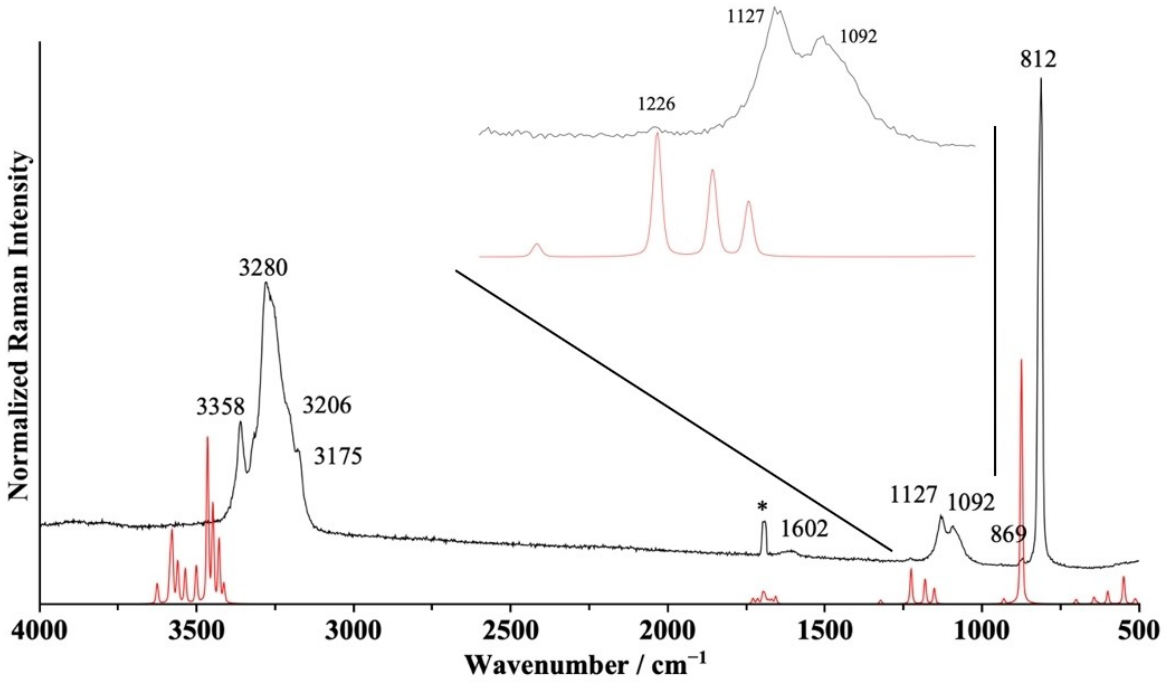

Figure 5. Recorded (top, black) and calculated (bottom, red) Raman spectrum of $[Tl_2(NH_3)_6][\{UO_2F_2(NH_3)\}_2(\mu\text{-}F)_2]$. The measured spectrum was obtained at room temperature with a 488 nm laser through the glass wall of a bomb tube. The Raman band caused by the 488 nm laser is marked with an asterisk. All wavenumbers correspond to the recorded Raman spectrum.

Research Article
doi.org/10.1002/ejic.202300387

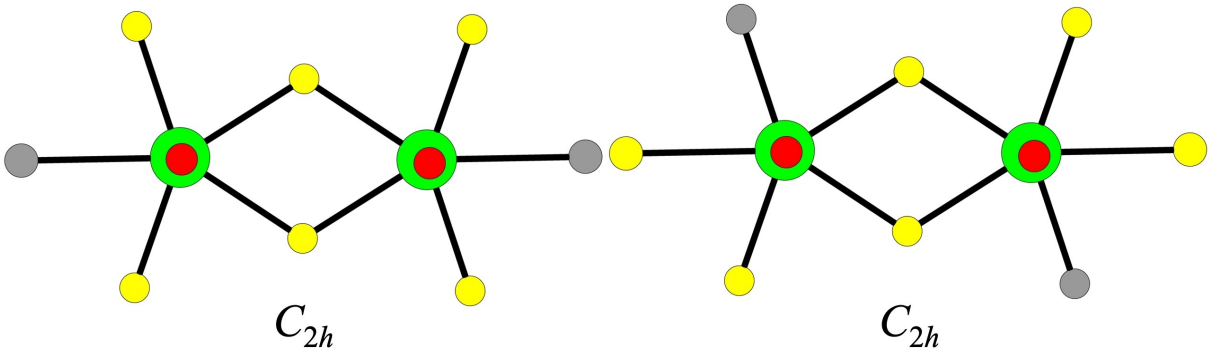

Figure 6. Different isomers of the complex anion. Idealized point group given underneath each structure. Left: F-*trans*-isomer with *trans*-NH_3/H_2O-ligands, the experimentally observed structure of the $[\{UO_2F_2(NH_3)\}_2(\mu\text{-}F)_2]^{2-}$ anion. Right: F-*cis*-isomer with *trans*-NH_3/H_2O-ligands, experimentally observed structure of the $[\{UO_2F_2(H_2O)\}_2(\mu\text{-}F)_2]^{2-}$ anion.[23] F atoms in yellow, U atoms in green, O atoms in red color. The ligands NH_3 or H_2O are shown in grey color.

The energy difference between the between the *trans* and *cis* isomer of the $[\{UO_2F_2(NH_3)\}_2(\mu\text{-}F)_2]^{2-}$ anion is only 1 kJ·mol^{-1} at the DFT-PBE0/TZVP level of theory, suggesting them to be practically isoenergetic.

The importance of the aqueous chemistry of the UO_2^{2+} cation has already been highlighted in the introduction. To compare the binding energies of the H_2O and NH_3 ligands, we studied the energetics of the ligand exchange reaction shown in Equation (3).

$$[\{UO_2F_2(NH_3)\}_2(\mu\text{-}F)_2]^{2-} + 2\ H_2O \rightleftharpoons [\{UO_2F_2(H_2O)\}_2(\mu\text{-}F)_2]^{2-} + 2\ NH_3 \quad (3)$$

The energetics were calculated within the idealized point group C_{2h} of the experimentally observed structures for the respective anion. Solvent effects were not explicitly considered in the calculation, but COSMO solvation model was used. The ligand exchange energy was calculated to be 23 kJ·mol^{-1}, meaning that the left side of Equation (3) is energetically more favorable. If Gibbs Free Energies are considered, the energy of the exchange reaction remains endothermic with $\Delta G =$ 19 kJ·mol^{-1} at room temperature. The DFT calculations thus suggest that there is a (weak) preference towards NH_3 ligand compared to the H_2O ligand. These findings are in line with previous calculations for the exchange of NH_3 ligands with H_2O ligands in the $[UO_2(NH_3)_5]^{2+}$ cation, where the ligand exchange energy at the DFT–B3LYP/6-311G+(d,p) level of theory was calculated to be 87 kJ·mol^{-1} favoring the $[UO_2(NH_3)_5]^{2+}$ cation.[9] All other possible permutations of ligands, the other different isomers, and exchange reactions are given in the Supporting Information.

A molecule with a bridging μ-F atom between two UO_2^{2+} units is uncommon, so we decided to investigate its bonding situation. We carried out DFT-PBE0/def2-TZVP calculations on the $[\{UO_2F_2(NH_3)\}_2(\mu\text{-}F)_2]^{2-}$ anion (C_{2h}) and performed a consecutive analysis of the intrinsic bond orbitals (IBOs).[27] The U–(μ-F)–U bond can be described best as a σ-3c-4e-bond. There are four of these σ-3c-4e-IBOs, from which two are shown in Figure 7. Due to numerical issues in the localization procedure, the localization of the wavefunction has been done in point group C_1, resulting in slightly different contributions of the U atoms.

Due to the high F atom contribution of 91 % and 90 %, the U–(μ-F)–U bond is very ionic nature, see the IBOs in Figure 7. The partial charges of the U atoms are +1.23 e^- and the partial charge of the μ-F atoms is −0.51 e^-. These values are essentially similar in comparison to the $[\{UO_2F_2(H_2O)\}_2(\mu\text{-}F)_2]^{2-}$ anion with +1.26 e^- for the U atom and −0.51 e^- for the μ-F atoms. For the first set of U–(μ-F)–U IBOs, the contributions of the U atoms with 4–5 % are dominated by the 6d orbital with 57 %, followed

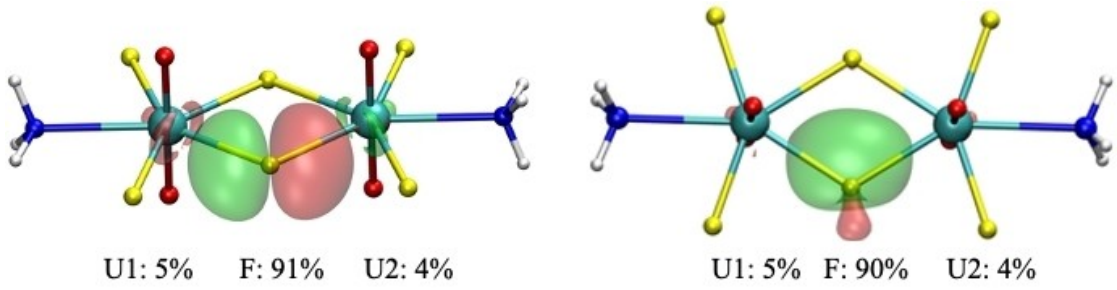

Figure 7. Two sets of IBOs for the $[\{UO_2F_2(NH_3)\}_2(\mu\text{-}F)_2]^{2-}$ anion (isosurfaces drawn in green and red). Left: One of two IBOs showing a σ-type bond between U–(μ-F)–U. Right: One of two IBOs showing the second σ-type bond between U–(μ-F)–U. The listed percentages show the contribution of each atom in the IBO. In a purely covalent 2c-bond, each atom would contribute 50 %. Atomic contributions smaller than 2 % to any IBO are not listed. The isovalue for IBO isosurface plots is 0.03 a.u. U atoms in cyan, N atoms in blue, O atoms in red, F atoms in yellow, and H atoms in white color.

Research Article
doi.org/10.1002/ejic.202300387

by the 5f orbital with 28%. The 7s orbital contributes with 17%. The contribution of the F atom arises completely from its 2p orbital. To the second set of IBOs, the U atoms contribute with 4–5%, with contributions of 66%, 18%, and 14% from 6d, 7s, and 5f orbitals, respectively. The F atoms have a mixed contribution of 56% 2s and 44% 2p orbital.

No values for the fluoride ion affinity (FIA) of the UO_2^{2+} cation have been reported as of yet. We studied the FIAs with the CCSD(T) method using the COF_2-system as a reference, see Experimental for computational details.[28] The conductor-like screening model approach (COSMO) was used for the HF reference wavefunction to counter the charges. The FIAs were calculated for the complexes $[UO_2F_x]^{2-x}$ and $[UO_2F_x(NH_3)_{5-x}]^{2-x}$ with $x=0$ to 4. Equations 4, 5, and 6 show the FIAs of the $[UO_2F_x(NH_3)_{5-x}]^{2-x}$ complexes with $x=0$ to 2, as they are of particular interest for the formation of the title anion, which can be seen as two $[UO_2F_3(NH_3)]^-$ fragments. All other calculated FIAs are given in the Supporting Information.

$$[UO_2(NH_3)_5]^{2+} + F^- \rightarrow [UO_2F(NH_3)_4]^+ + NH_3;\ \mathrm{FIA} = -216\ \mathrm{kJ\cdot mol^{-1}} \quad (4)$$

$$[UO_2F(NH_3)_4]^+ + F^- \rightarrow [UO_2F_2(NH_3)_3] + NH_3;\ \mathrm{FIA} = -193\ \mathrm{kJ\cdot mol^{-1}} \quad (5)$$

$$[UO_2F_2(NH_3)_3] + F^- \rightarrow [UO_2F_3(NH_3)_2]^- + NH_3;\ \mathrm{FIA} = -169\ \mathrm{kJ\cdot mol^{-1}} \quad (6)$$

The calculated FIAs of the species involved in Equations (4), (5), and (6) range in the area of medium to strong acceptors, when compared to SbF_5 with a calculated value of 489 $kJ\cdot mol^{-1}$ (439 $kJ\cdot mol^{-1}$ COSMO corrected).[28,29] These values are in line with our calculations using the CCSD(T) method for SbF_5, 496 versus 432 $kJ\cdot mol^{-1}$, see Supporting Information for more details. COSMO has a significant effect on the FIAs, and it has been suggested that it affects FIAs with errors between 100 and 400 $kJ\cdot mol^{-1}$ for cationic species.[30] With that considered the uranyl(VI) ammine species become strong fluoride ion acceptors with respect to SbF_5. For UO_2^{2+}, the FIA is as large as $-394\ kJ\cdot mol^{-1}$. However, the FIAs of anions $[UO_2F_3]^{2-}$ and $[UO_2F_4]^{3-}$become positive with $+16$ and $+134\ kJ\cdot mol^{-1}$, respectively, possibly due to Coulombic repulsion.

Conclusions

The reaction of UO_2F_2 with TlF strongly points in the direction of UO_2F_2 being a F^- anion acceptor in liquid ammonia as the compound $[Tl_2(NH_3)_6][\{UO_2F_2(NH_3)\}_2(\mu\text{-}F)_2]$ was formed. The $[Tl_2(NH_3)_6]^{2+}$ cation shows a thallophilic interaction. A quantum-chemical investigation of the $[\{UO_2F_2(NH_3)\}_2(\mu\text{-}F)_2]^{2-}$ anion showed that the μ-F atoms have an essentially ionic character, as their contributions to the Intrinsic Bonding Orbitals of the U−(μ-F)−U σ-3c-4e-bond are 90% or larger.

The $[\{UO_2F_2(NH_3)\}_2(\mu\text{-}F)_2]^{2-}$ anion is a good example of the comparability of liquid aNH_3 being an aqueous-like solvent, as the related aqua complex $[\{UO_2F_2(H_2O)\}_2(\mu\text{-}F)_2]^{2-}$ has already been reported. However, the solvato ligands are bound differently leading to coordination isomers. A study of the energetics of the ligand exchange reaction of H_2O versus NH_3 using the experimentally observed structures showed that the NH_3 ligand is favored by 20 $kJ\cdot mol^{-1}$. The permutation of different coordination isomers has no effect on the energy of the exchange reaction of the NH_3 ligands by H_2O ligands. Also, the consideration of Gibbs Free Energies did not change the situation.

The calculated FIAs for the ammine complexes support the idea that the UO_2^{2+} cation is a strong F^- acceptor, with a calculated FIA of $-216\ kJ\cdot mol^{-1}$ for the $[UO_2(NH_3)_5]^{2+}$ cation. For the UO_2^{2+} cation without additional ammine ligands bound, the FIA was calculated to be even stronger with 394 $kJ\cdot mol^{-1}$ which is close to the very strong Lewis acid SbF_5 with 495 $kJ\cdot mol^{-1}$.

Experimental Section

All work was carried out under argon atmosphere (5.0, Praxair) using a fine vacuum line and a glovebox (MBraun). Liquid ammonia was dried by storage over Na. The self-made borosilicate glass bomb tubes for reactions in liquid ammonia were flame-dried at least three times under vacuum. UO_2F_2 was prepared according to the literature in a slightly adapted procedure from $(UO_2)(O_2)\cdot 2H_2O$ and anhydrous HF.[31] Uranium compounds are radioactive, and appropriate/required measures for safe handling need to be taken. HF may pose a working hazard to those being unexperienced, untrained, or unskilled. Suitable protective gear should be worn at all times and access to proper medical treatment is necessary.

Preparation of $[Tl_2(NH_3)_6][\{UO_2F_2(NH_3)\}_2(\mu\text{-}F)_2]$

A borosilicate bomb tube was charged with 82 mg UO_2F_2 (0.28 mmol) and 66 mg TlF (0.28 mmol, 1 eq.), filled with approximately 2 mL liquid NH_3 then flame-sealed and stored at 40 °C. After 10 months yellow crystals were observed and large enough for a Raman measurement and then grown large enough for X-ray diffraction experiments. After removal of residual liquid NH_3, an orange powder remained.

Raman spectroscopy

The Raman spectra were measured at room temperature with a Monovista CRS+ confocal Raman microscope (Spectroscopy & Imaging GmbH) using a solid-state laser with $\lambda=488$ nm and a 300 grooves/mm (low-resolution mode, FWHM: $<5.50\ cm^{-1}$) grating.

IR spectroscopy

The IR spectrum was recorded on a Bruker alpha FT-IR spectrometer using the ATR Diamond module with a resolution of 4 cm^{-1}. The spectrometer was located inside a glovebox (MBraun) under argon atmosphere. The spectra were processed with the OPUS software package.[32]

Research Article
doi.org/10.1002/ejic.202300387

Single crystal X-ray diffraction

The crystals of the compound $[Tl_2(NH_3)_6][\{UO_2F_2(NH_3)\}_2(\mu\text{-}F)_2]$ were selected under nitrogen-cooled, pre-dried perfluorinated oil under the exclusion of air. The crystals were mounted with a MiTeGen loop. Intensity data of a suitable crystal were recorded with a D8 Quest diffractometer (Bruker). The diffractometer was operated with monochromatized Mo-K_α radiation (0.71073 Å, multi layered optics) and equipped with a PHOTON 100 CMOS detector. Evaluation, integration, and reduction of the diffraction data was carried out with the APEX3 software suite.[33] The diffraction data were corrected for absorption utilizing the multi-scan method of SADABS within the APEX3 software suite. The structure was solved with dualspace methods (SHELXT) and refined against F^2 (SHELXL).[34,35] All atoms were refined with anisotropic displacement parameters, H atoms were refined isotropic with a riding model. Representations of the crystal structure were created with the Diamond software.[36] Further details are discussed in the Supporting Information. Deposition Number 2270898 contains the supplementary crystallographic data for this paper. These data are provided free of charge by the joint Cambridge Crystallographic Data Centre and Fachinformationszentrum Karlsruhe Access Structures service.

Powder X-ray diffraction

The synthesized UO_2F_2 was filled into a flame-dried borosilicate glass capillary with a diameter of 0.3 mm. A sample of the orange left-overs obtained by warming $[Tl_2(NH_3)_6][\{UO_2F_2(NH_3)\}_2(\mu\text{-}F)_2]$ to room temperature was filled into a flame-dried borosilicate glass capillary with a diameter of 0.3 mm. The powder X-ray diffraction pattern was recorded with a StadiMP diffractometer (Stoe & Cie) in Debye-Scherrer geometry. The diffractometer was operated with $Cu_{K\alpha1}$ radiation (1.5406 Å, germanium monochromator) and equipped with a MYTHEN 1 K detector. The diffraction pattern was processed using the WinXPOW suite.[37]

Computational Details

Molecular DFT calculations were carried out with the TURBOMOLE7.7[38,39] program suite using the PBE0 hybrid density functional method (DFT-PBE0).[40,41] We used def2-TZVP triple-ζ valence basis sets for hydrogen, nitrogen, oxygen, and fluorine atoms.[42] For the uranium atom, scalar relativistic effects were taken into account using a 60-electron effective core potential (ECP) combined with def-TZVP triple-ζ valence basis set.[42–45] For the antimony atom, scalar relativistic effects were taken into account using a 28-electron effective core potential (ECP) combined with def2-TZVP triple-ζ valence basis set.[42,46] Multipole-accelerated resolution-of-the-identity approximation (MA-RIJ) was used to speed up the DFT calculations[47–49] and an m4 integration grid was used for the numerical integration of the exchange-correlation part. The "COnductor-like Screening MOdel" (COSMO) was applied to all structures to compensate the negative charges.[50] The structures of the complex anions were fully optimized within the constraints of their respective molecular point group symmetry. Numerical harmonic frequency calculations were performed to check if the optimized structures were true local minima on the potential energy surface. The coordinates of the optimized structures are available from the Supporting Information. Intrinsic bond orbital (IBO) analyses were performed with the Turbomole module *proper*.[27] Previously published U[51] reference basis set was used for the IBO analysis. Gibbs Free Energies were obtained within the harmonic oscillator rigid rotor model at room temperature, using the *freeh* module. The harmonic frequencies were not scaled when evaluating the thermal contributions.

For the *ab initio* coupled-cluster (CC) calculations, the Karlsruhe def2-QZVPP[52] basis sets were applied for the elements H, N, O, and F. For Sb, def2-QZVPP[42] basis set combined with the 60-electron scalar relativistic ECP was used. For U, def-TZVPP[43] basis set combined with the 60-electron scalar relativistic ECP was used. CC single-point energies were calculated for structures optimized at the DFT-PBE0/TZVP level of theory described above. The resolution of the identity (RI) approximation was used to speed up the CC calculations.[53] The RI auxiliary basis set for U was generated with the AutoAux feature of the Orca 5.0.3[54] program suite and used in the Turbomole calculations (basis set listing is available in the Supporting Information). Core orbitals were frozen in the CC calculations as follows: N, O, F: 1*s*; Sb: ECP contains 1*s*2*s*2*p*3*s*3*p*3*d* and 4*s*4p were frozen; U: ECP contains 1*s*2*s*2*p*3*s*3*p*3*d*4*s*4*p*4*d*4*f* and 5*s*5p5d were frozen.

Periodic quantum-chemical calculations were conducted using the CRYSTAL23 software suite.[55] The DFT-PBE0 hybrid density functional method (PBE + 25% exact HF exchange) was used in all calculations.[40,41] Gaussian-type triple-ζ-valence + polarization basis set TZVP were applied for all elements. The basis sets have been derived from the Karlsruhe basis sets and the U basis includes 60-electron scalar relativistic effective core potential.[44,56] The basis sets for U, H, N, O, and F have been published previously.[57,58] Full details on the Tl basis set are given in the Supporting Information. The crystal structure was fully optimized within the symmetry constrains of the space group. The reciprocal space was sampled with a 3 × 3 × 3 Monkhorst-Pack-type *k*-point grid.[59] Tight tolerances (TOLINTEG) of 8 8 8 8 16 were used to for the evaluation of the Coulomb and exchange integrals. Default optimization criteria and DFT integration grids of CRYSTAL23 were applied. The optimized lattice parameters deviated by less than 2% from the lattice parameters determined with SCXRD. The optimized crystal structure was confirmed to be true local minimum by means of harmonic frequency calculation.[60,61]

Supporting Information

The Supporting Information contains further crystallographic details, the powder X-ray diffraction pattern, details for the IR and Raman spectroscopies, details of the quantum-chemical calculations and the hydrogen bonding.[62–64]

Acknowledgements

T. G. thanks the HPC-EUROPA3 (INFRAIA-2016-1-730897) for a travel grant and the computing resources provided by CSC, the Finnish IT Center for Science. T. G. thanks A. Barba for conducting some experiments. F. K. thanks the Deutsche Forschungsgemeinschaft, KR3595/13-1, for funding. Open Access funding enabled and organized by Projekt DEAL.

Conflict of Interests

The authors declare no conflict of interest.

Data Availability Statement

The data that support the findings of this study are available in the supplementary material of this article.

Keywords: Uranium · uranyl fluoride · liquid ammonia · thallium · quantum-chemical calculations

[1] K. E. Knope, L. Soderholm, *Chem. Rev.* **2013**, *113*, 944–994.
[2] M. Altmaier, X. Gaona, T. Fanghänel, *Chem. Rev.* **2013**, *113*, 901–943.
[3] V. Doetsch, J. Jander, U. Engelhardt, C. Lafrenz, J. Fischer, H. Nagel, W. Renz, G. Türk, T. von Volkmann, G. Weber, in *Chemistry in Anhydrous Liquid Ammonia – Part 1 – Anorganische Und Allgemeine Chemie in Flüssigem Ammoniak*, Friedr. Vieweg & Sohn, Braunschweig, **1966**.
[4] W. Peters, *Z. Anorg. Allg. Chem.* **1912**, *77*, 137–190.
[5] P. Spacu, *Z. Anorg. Allg. Chem.* **1936**, *230*, 181–186.
[6] A. von Unruh, in *Einwirkung von Trockenem Ammoniak Auf Wasserfreie Uranylsalze*, Universität Rostock, **1909**.
[7] I. Kalnins, G. Gibson, *J. Inorg. Nucl. Chem.* **1959**, *11*, 115–123.
[8] P. Woidy, A. J. Karttunen, F. Kraus, *Z. Anorg. Allg. Chem.* **2012**, *638*, 2044–2052.
[9] P. Woidy, M. Bühl, F. Kraus, *Dalton Trans.* **2015**, *44*, 7332–7337.
[10] P. Woidy, F. Kraus, *Acta Crystallogr. Sect. E* **2016**, *72*, 1710–1713.
[11] Z. Szabó, J. Glaser, I. Grenthe, *Inorg. Chem.* **1996**, *35*, 2036–2044.
[12] G. H. John, I. May, D. Collison, M. Helliwell, *Polyhedron* **2004**, *23*, 3097–3103.
[13] J. Fawcett, J. H. Holloway, D. Laycock, D. R. Russell, *J. Chem. Soc. Dalton Trans.* **1982**, 1355–1360.
[14] F. Kraus, *BioInorganic React. Mech.* **2012**, *8*, 29–39.
[15] E. C. Franklin, C. A. Kraus, *Am. Chem. J.* **1898**, *20*, 820–853.
[16] W. Biltz, E. Rahlfs, *Z. Anorg. Allg. Chem.* **1927**, *166*, 351–376.
[17] J. C. Dougal, P. Gans, J. B. Gill, L. H. Johnson, *Pure Appl. Chem.* **1988**, *60*, 1731–1742.
[18] J. J. Lagowski, *Synth. React. Inorg. Met.-Org. Nano-Met. Chem.* **2007**, *37*, 115–153.
[19] P. Woidy, A. J. Karttunen, S. S. Rudel, F. Kraus, *Chem. Commun.* **2015**, *51*, 11826–11829.
[20] S. S. Rudel, T. Graubner, A. J. Karttunen, S. Dehnen, F. Kraus, *Inorg. Chem.* **2021**, *60*, 15031–15040.
[21] S. S. Rudel, S. A. Baer, P. Woidy, T. G. Müller, H. L. Deubner, B. Scheibe, F. Kraus, *Z. Kristallogr.* **2018**, *233*, 817–844.
[22] Y. N. Mikhailov, S. B. Ivanov, G. G. Sadikov, *Koord. Khim.* **1979**, *5*, 1702–1705.
[23] Yu. N. Mikhailov, S. B. Ivanov, A. A. Udovenko, R. L. Davidovich, V. G. Kuznetsov, V. V. Peshkov, *J. Struct. Chem.* **1975**, *15*, 838–839.
[24] S. Jamet, N. Q. Dao, J.-C. Morlaes, *C. R. Hebd. Seances Acad. Sci., Ser. C* **1975**, *281*, 593–596.
[25] L. L. Zaitseva, L. V. Lipis, V. V. Fomin, N. T. Chebotarev, *Zh. Neorg. Khim.* **1962**, *7*.
[26] H. Brusset, N. Q. Dao, *C. R. Seances Acad. Sci. Ser. C* **1970**, *271*, 303–306.
[27] G. Knizia, *J. Chem. Theory Comput.* **2013**, *9*, 4834–4843.
[28] P. Erdmann, J. Leitner, J. Schwarz, L. Greb, *ChemPhysChem* **2020**, *21*, 987–994.
[29] J. M. Slattery, S. Hussein, *Dalton Trans.* **2012**, *41*, 1808–1815.
[30] L. Greb, *Chem. Eur. J.* **2018**, *24*, 17881–17896.
[31] M. C. Chakravorti, M. Chowdhury, P. G. Eller, R. J. Kissane, *Inorg. Synth.* **1989**, *25*, 144–146.
[32] *OPUS V7.2*, Bruker Optik GmbH, Ettlingen, Germany, **2012**.
[33] *APEX3 V2019.11-2*, Bruker AXS Inc., Madison, Wisconsin, USA, **2019**.
[34] G. M. Sheldrick, *Acta Crystallogr. Sect. A* **2015**, *71*, 3–8.
[35] G. M. Sheldrick, *Acta Crystallogr. Sect. C* **2015**, *71*, 3–8.
[36] K. Brandenburg, H. Putz, in *Diamond – Crystal and Molecular Structure Visualization, V 4.6.8*, Crystal Impact GbR, Bonn, **2022**.
[37] *WinXPOW V3.11*, STOE, Darmstadt, Germany, **2018**.
[38] R. Ahlrichs, M. Bär, M. Häser, H. Horn, C. Kölmel, *Chem. Phys. Lett.* **1989**, *162*, 165–169.
[39] *TURBOMOLE V7.7, a Development of University of Karlsruhe and Forschungszentrum Karlsruhe GmbH, 1989–2007, TURBOMOLE GmbH, since 2007*. **2022**.
[40] C. Adamo, V. Barone, *J. Chem. Phys.* **1999**, *110*, 6158–6170.
[41] J. P. Perdew, K. Burke, M. Ernzerhof, *Phys. Rev. Lett.* **1996**, *77*, 3865–3868.
[42] F. Weigend, R. Ahlrichs, *Phys. Chem. Chem. Phys.* **2005**, *7*, 3297–3305.
[43] A. Schäfer, C. Huber, R. Ahlrichs, *J. Chem. Phys.* **1994**, *100*, 5829–5835.
[44] W. Küchle, M. Dolg, H. Stoll, H. Preuss, *J. Chem. Phys.* **1994**, *100*, 7535–7542.
[45] X. Cao, M. Dolg, H. Stoll, *J. Chem. Phys.* **2003**, *118*, 487–496.
[46] A. Bergner, M. Dolg, W. Küchle, H. Stoll, H. Preuß, *Mol. Phys.* **1993**, *80*, 1431–1441.
[47] F. Weigend, *Phys. Chem. Chem. Phys.* **2002**, *4*, 4285–4291.
[48] K. Eichkorn, O. Treutler, H. Öhm, M. Häser, R. Ahlrichs, *Chem. Phys. Lett.* **1995**, *240*, 283–290.
[49] M. Sierka, A. Hogekamp, R. Ahlrichs, *J. Chem. Phys.* **2003**, *118*, 9136–9148.
[50] A. Klamt, G. Schürmann, *J. Chem. Soc. Perkin Trans. 2* **1993**, 799–805.
[51] S. S. Rudel, H. L. Deubner, M. Müller, A. J. Karttunen, F. Kraus, *Nat. Chem.* **2020**, *12*, 962–967.
[52] F. Weigend, F. Furche, R. Ahlrichs, *J. Chem. Phys.* **2003**, *119*, 12753–12762.
[53] A. Hellweg, C. Hättig, S. Höfener, W. Klopper, *Theor. Chem. Acc.* **2007**, *117*, 587–597.
[54] F. Neese, *WIREs Comput. Mol. Sci.* **2022**, *12*, e1606.
[55] A. Erba, J. K. Desmarais, S. Casassa, B. Civalleri, L. Donà, I. J. Bush, B. Searle, L. Maschio, L. Edith-Daga, A. Cossard, C. Ribaldone, E. Ascrizzi, N. L. Marana, J.-P. Flament, B. Kirtman, *J. Chem. Theory Comput.* **2022**, acs.jctc.2c00958.
[56] X. Cao, M. Dolg, *J. Mol. Struct.: THEOCHEM* **2004**, *673*, 203–209.
[57] S. S. Rudel, A. J. Karttunen, F. Kraus, *Z. Anorg. Allg. Chem.* **2020**, *646*, 1023–1029.
[58] A. J. Karttunen, T. Tynell, M. Karppinen, *J. Phys. Chem. C* **2015**, *119*, 13105–13114.
[59] H. J. Monkhorst, J. D. Pack, *Phys. Rev. B* **1976**, *13*, 5188–5192.
[60] R. Dovesi, A. Erba, R. Orlando, C. M. Zicovich-Wilson, B. Civalleri, L. Maschio, M. Rérat, S. Casassa, J. Baima, S. Salustro, B. Kirtman, *Wiley Interdiscip. Rev.: Comput. Mol. Sci.* **2018**, *8*, e1360.
[61] F. Pascale, C. M. Zicovich-Wilson, F. López Gejo, B. Civalleri, R. Orlando, R. Dovesi, *J. Comput. Chem.* **2004**, *25*, 888–897.
[62] H. T. Stokes, D. M. Hatch, *J. Appl. Crystallogr.* **2005**, *38*, 237–238.
[63] G. Gilli, P. Gilli, *The Nature of the Hydrogen Bond*, Oxford University Press, Oxford, **2009**.
[64] S. Alvarez, *Dalton Trans.* **2013**, *42*, 8617–8636.

Manuscript received: June 19, 2023
Revised manuscript received: July 17, 2023
Accepted manuscript online: July 18, 2023
Version of record online: August 1, 2023